Publisher: Engineering College, Al Muthanna University

Open Access

DOI:10.52113/3/eng/mjet/2025-13-03-/1-14, Vol. (13), Issue (3), (2025)

Muthanna Journal of Engineering and Technology MJET

Submitted 20 June 2025, Accepted 18 August 2025, Published online 1 September 2025

Dynamic Simulation of Phase Change Material-Integrated Solar Water Heating Systems: A Machine Learning Approach to Energy Conversion Optimization

Falah A. Barqawi

Babol Noshirvany University of Technology

albarqawyfalah@gmail.com

Abstract

Phase change material (PCM) integrated solar water heating systems represent a critical technology for sustainable energy applications, yet face significant performance limitations due to poor thermal conductivity and lack of intelligent control optimization. This study aims to develop and validate a novel machine learning-driven optimization control technique for PCM-based solar water heating systems. The methodology employs a comprehensive three-phase mathematical model encompassing pre-melting, melting transition, and post-melting thermal dynamics, coupled with a neural network controller operating on real-time environmental data to predict optimal pump flow multipliers. Comprehensive simulation validation across five environmental conditions and three PCM materials demonstrated consistent performance improvements with energy storage enhancements of 2.5-4.1% (3.3% average) and heat transfer enhancement ratios of 1.03-1.04×. This research provides the first complete ML-based control system for PCM thermal energy storage with retrofit-compatible optimization requiring no hardware modifications, offering a quantifiable performance benefit for existing installations.

Keywords: *Intelligent Control; Machine Learning Optimization; Phase Change Materials; Renewable Energy Systems; Solar Water Heating.*

1. Introduction

The world's energy situation is unprecedented, with rising energy needs coming in line with climate change mitigation imperatives, necessitating an accelerated transition to sustainable energy systems. The International Energy Agency estimates the share of buildings in world energy consumption to be around 40% [1], of which space heating and domestic hot water are the largest end-use applications [2]. This strong demand, coupled with the context and volatile prices of fossil fuels, has driven research and development (R&D) in renewable energy technologies with efficient, cost-effective alternatives to conventional heating technologies [2]. Solar thermal energy has been a well-established, low-cost technology to meet building thermal needs, and more than 500 GW thermal capacity installations have been implemented globally as of 2023 [3].

Solar water heaters are among the most effective proven renewable energy technologies with measurable performance under different climatic conditions around the globe. Solar radiation intermittence is, however, a serious problem in ensuring a steady thermal energy supply, particularly at low irradiance or night operations [4]. Traditional systems have faced time mismatches between supply and demand of energy, having a tendency to be overdimensioned for collector areas or backup heaters in order to be acceptably performing [5]. These limitations have spurred extensive research activities in thermal energy storage (TES) technologies with the potential to efficiently absorb, store, and release thermal energy in order to bridge the gap between the availability of solar energy and users' demand patterns [6].

Phase change materials (PCM) are particularly promising for latent heat thermal energy storage since they can store high capacities of thermal energy at low temperature ranges through solid-liquid phase change. Compared to sensible heat storage systems with cyclical temperature changes in charging and discharging operations, PCM-based systems have comparatively stable temperatures during phase changes with better thermal stability and energy storage density [7]. The breakthroughs demonstrate energy storage densities of 150-250 kJ/kg for organic compounds and 300-400 kJ/kg for inorganic compounds, which are huge advances over conventional sensible heat storage media [8]. Applications of PCM in solar thermal systems can reduce collector area needs by 20-30% with comparable thermal performance, improving system economics overall [9].

Despite such advantages, PCM-based thermal energy storage systems have technical shortcomings that can hinder widespread commercialization. Relatively low thermal conductivity of most potential PCM materials (commonly 0.1-0.5 W/m·K) causes unfavorable heat transfer behavior and long charging/discharging time, resulting in poor system responsiveness [10]. Challenges such as supercooling of inorganic PCMs, thermal degradation in cycling, and encapsulation of organic material remain key engineering issues [11]. Most of the work at present is material-level enhancement, i.e., dispersion of nanoparticles, embedding of metal foam, and cutting-edge encapsulation techniques, which exhibit excellent performance at traditionally high added cost and complexity [12].

Machine learning and intelligent control systems in thermal energy systems have also picked up speed due to advances in computing power, sensor networks, and data analytics [13]. Machine learning algorithms have succeeded in optimizing building energy systems with 10-30% energy savings reported by smart heating, ventilation, and air conditioning (HVAC) control, predictive maintenance, and demand response optimization [14]. However, machine learning deployment to PCM thermal energy storage optimization is remarkably underutilized, and it is a massive research opportunity. The nonlinear, multivalued nature of PCM system thermal dynamics and highly variable environmental conditions create the ideal set of circumstances for machine learning-based optimization techniques that are capable of optimally operating systems in real time to prevailing conditions and established patterns of performance [15].

This paper fills the research gap by developing and verifying a novel machine learning-informed control optimization strategy for PCM-integrated solar water heaters. The study investigates the dynamic thermal response of PCM materials under different environmental conditions, comparing conventional fixed-speed pump control with variable-speed smart optimization strategies. The study involves analytical mathematical modeling of three-phase PCM thermal dynamics, developing and training neural network-based control algorithms, and rigorous simulation-based verification across different operating conditions.

The significant contributions include the design of the machine learning-based control optimization approach for PCM-integrated solar water heaters, the design of the complete three-phase mathematical model representing pre-melting, melting transition, and post-melting thermal behaviors, comprehensive evaluation under five various environmental conditions, and design of a retrofit-compatible optimization technique with only software adjustments and slight sensing hardware. The study provides reproducible quantitative performance assessment with energy storage improvements of 2.5-4.1% for various PCM materials, indicating that very high performance improvement can be achieved through control optimization alone while augmenting existing physical enhancement methods.

2. Related Work

Development of phase change material (PCM) thermal energy storage systems is a focused research area with studies focusing on improving heat transfer characteristics, energy storage capacity, and system performance. Three methods of improvement are emphasized in the literature: physical upgrading, geometry design improvement, and system integration techniques. However, significant focus has been on intelligent control optimization methods, suggesting a knowledge gap that this work attempts to bridge.

Modification of nanoparticles is the most studied physical modification technique in current PCM investigations. Dayer et al. (2024) [16] conducted experimental work on improving thermal performance by using Al_2O_3 nanoparticles in PVT water harvesting systems and attaining up to 32% thermal conductivity improvements with associated electrical (14%) and thermal efficiency (72%) increases in the laboratory setting. Optimum concentrations are 0.5% to 2% weight, and nanoparticle dispersion homogeneity and concentration are crucial factors. Tamizharasan et al. (2024) [17] explored silicon carbide (SiC) nanoparticle addition to PCM/PVT systems with similar efficiency improvement while addressing long-term nanoparticle settling stability issues. These studies demonstrate significant performance improvement but cite implementation issues like high material costs, potential agglomeration, and complex manufacturing processes.

Other physical enhancement techniques aim at low-cost industrial substitutes. Prieto et al. (2021) [18] proposed metal wool infiltration to enhance PCM thermal conductivity in high-temperature solar process heat applications (150-500°C), with a maximum of 4.34 W/m·K conductance improvement over conventional organic PCM materials with less than 1 W/m·K conductivity. Yousef et al. (2020) [19] empirically confirmed metal wool enhancement for solar still latent heat storage

systems with 25% productivity improvement. Metal wool enhancement has the benefits of material costs and scalability of production, particularly for industrial use in mass production. Geometric enhancement techniques are substitute methods to material enhancements. Vempally et al. (2024) [20] studied the solidification behavior of copper-water nanofluids in wavy-wall enclosures and demonstrated that surface waviness controls the solidification times and enhances heat transfer performance. Numerical modeling showed sinusoidal wavy wall geometries achieved 30-80% melting time reductions compared to flat-wall geometries, where the gain depended on wave amplitude and frequency parameters.

Literature review suggests that while tremendous strides have been made in physical and geometric improvement methods, software optimization potential remains largely unexploited. Current improvement methods require huge capital expenses, sophisticated high-technology manufacturing process steps, or complete system redesigns that limit applicability to installed equipment. Research motivation is provided by this demand. Intelligent control approaches that provide substantial performance gains based on software modifiability alone, along with retrofit compatibility and cost economies, are developed. The machine learning optimization strategy presented here is a new PCM improvement contribution that addresses real-world deployment issues while guaranteeing quantifiable performance enhancements over general operating conditions.

3. Methodology

3.1 Dataset Description and System Parameters

The comprehensive simulation study utilized a well-chosen dataset of five various phase change materials (PCM) and different environmental conditions for comparing the thermal performance of solar water heating systems. Figure 1. displays the system design and key parameters utilized in this study.

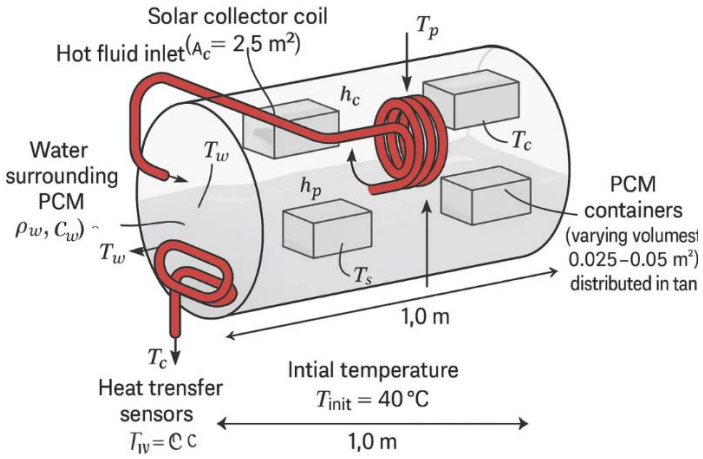

Fig. 1: Schematic diagram of PCM-integrated solar water heating system with component specifications [Adapted from 21].

Table 1 provides a summary of the full thermophysical properties and system parameters of all the PCM materials used in this study.

Table 1: PCM Material Properties and System Parameters

Parameter	P01	P02	P03	P04	P05	Unit
PCM Properties						
Melting Temperature (Tmelt)	44.0	44.0	44.0	44.0	44.0	°C
Solid Specific Heat (C_ps)	2100	2100	2100	2100	2100	J/kg·K
Liquid Specific Heat (C_pl)	2300	2300	2300	2300	2300	J/kg·K
Heat of Fusion (Hf)	165000	165000	165000	165000	165000	J/kg
Density (ρ_p)	850	850	850	850	850	kg/m³
System Configuration						
Tank Length (L)	1.0	1.0	1.0	1.0	1.0	m
Tank Diameter (diam)	0.5	0.5	0.5	0.5	0.5	m
PCM Volume (Vp)	0.05	0.03	0.025	0.025	0.035	m³
PCM Surface Area (Ap)	5.0	3.0	2.5	2.5	3.5	m²
Heat Transfer Parameters						
Coil Area (Ac)	2.5	2.5	2.5	2.5	2.5	m²
Water-Coil HTC (hc)	1500	1500	1500	1500	1500	W/m²·K
PCM-Water HTC (hp)	800	800	800	800	800	W/m²·K
Operating Conditions						
Initial Temperature (Tinit)	40.0	40.0	40.0	40.0	40.0	°C

Simulation Duration (tfinal)	50400	50400	50400	50400	50400	s
Time Step (tstep)	100	100	100	100	100	s

The heat transfer coefficients hc and hp represent forced convection conditions calculated using the Dittus-Boelter correlation for turbulent flow in pipes, with values determined based on typical water flow rates of 0.02-0.05 m/s and Reynolds numbers in the range of 2000-5000 [26].

The environmental data set comprises five distinct scenarios created to portray the variation in solar irradiance and ambient conditions: Summer Sunny (high irradiance, favorable conditions), Winter Cloudy (low irradiance, unfavorable conditions), Summer Variable (variable irradiance), Winter Sunny (medium irradiance, low ambient temperature), and Summer Cloudy (reduced irradiance, moderate ambient temperature). Each scenario incorporates realistic solar irradiance profiles, ambient temperature variations, and seasonal effects to enable comprehensive system testing under diverse operating conditions.

It should be noted that the PCM materials P01-P05 differ only in system configuration parameters (volume, surface area) while maintaining identical thermophysical properties, allowing for comparative analysis of geometric effects on thermal performance.

Table 2: Environmental Scenario Parameters [27]

Scenario	Peak Irradiance (W/m²)	Seasonal Factor	Efficiency	Ambient Temperature (°C)	Duration (hours)
Summer Sunny	800	1.0	0.7	25	14
Winter Cloudy	400	0.7	0.5	15	14
Summer Variable	600	1.0	0.6	22	14
Winter Sunny	600	0.7	0.65	18	14
Summer Cloudy	500	1.0	0.55	23	14

3.2 Mathematical Modeling Framework

The thermo-dynamic performance of the solar water heating system with PCM is governed by a general set of differential equations modeling the dynamic heat transfer processes, phase change, and system interactions. The mathematical model is developed according to three stages of operation of the PCM: pre-melting (solid state), melting transition, and post-melting (liquid state).

The mathematical model assumes no external heating load during simulation periods, focusing on energy storage performance under solar input conditions. Heat losses to ambient environment are neglected to isolate the PCM enhancement effects.

Phase 1: Pre-Melting Dynamics

During the initial heating phase, when the PCM temperature is below the melting point, the system dynamics are modeled by the following system of coupled ordinary differential equations: [22]

$$\frac{dTw}{dt} = \left(\frac{1}{\tau w}\right) \times [(Tc(t) - Tw) + \eta \times (Tp - Tw)] \quad (1)$$

$$\frac{dTp}{dt} = \left(\frac{1}{\tau ps}\right) \times (Tw - Tp) \quad (2)$$

Where:

- Tw and Tp are water and PCM temperatures, respectively
- $Tc(t)$ is the coil temperature with time dependence according to solar irradiance
- $\tau w = (Mw \times Cw)/(hc \times Ac)$ is the water thermal time constant
- $\tau ps = (Mp \times Cps)/(hp \times Ap)$ is the solid PCM thermal time constant
- $\eta = (hp \times Ap)/(hc \times Ac)$ is the heat transfer coupling parameter

The dynamic coil temperature is calculated based on solar input parameters: [23] [24]

$$Tc(t) = Tamb + \frac{efficiency \times I_{solar(t)}}{20} \quad (3)$$

$$Isolar(t) = Imax \times \sin\left(\pi \times \frac{t\ hours - sunrise}{sunset - sunrise}\right) \quad (4)$$

where sunrise and sunset times are calculated for a reference location at 33°N latitude, 44°E longitude (representative of Middle Eastern climate conditions).

Phase 2: Melting Transition

As the PCM temperature increases to the melting point ($Tmelt$), the phase change zone is entered by the system, a zone of isothermal heat absorption. The equations governing the system are now:

$$\frac{dTw}{dt} = \left(\frac{1}{\tau w}\right) \times [(Tc(t) - Tw) + \eta \times (Tmelt - Tw)] \quad (5)$$

$$\frac{dTp}{dt} = 0 \quad (6)$$

$$\frac{dQp}{dt} = hp \times Ap \times \max(0, (Tw - Tmelt)) \quad (7)$$

where Qp is the total latent heat energy stored during melting. The melting phase continues until the total latent heat capacity is reached:

$$Qp, max = Hf \times Mp \quad (8)$$

Phase 3: Post-Melting Dynamics

Once the phase change process is over, the system moves into liquid PCM operation with changed thermal properties:

$$\frac{dTw}{dt} = \left(\frac{1}{\tau w}\right) \times [(Tc(t) - Tw) + \eta \times (Tp - Tw)] \quad (9)$$

$$\frac{dTp}{dt} = \left(\frac{1}{\tau pl}\right) \times (Tw - Tp) \quad (10)$$

where $\tau pl = (Mp \times Cpl)/(hp \times Ap)$ is the liquid PCM's thermal time constant, incorporating the different liquid phase specific heat capacity. Figure 2. describes the three-phase modeling approach with automatic phase transition detection.

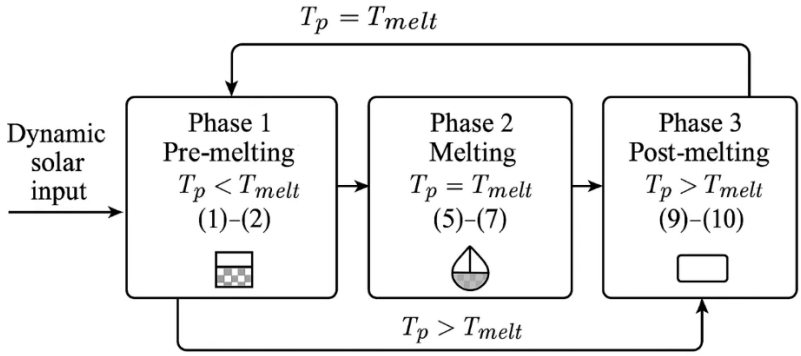

Fig. 2: Three-phase mathematical modeling framework for PCM thermal dynamics.

3.3 Energy Balance Calculations

The system's overall energy balance encompasses both the latent and sensible heat storage terms:

Phase 1 Energy (Pre-melting):

$$EWater = Cw \times Mw \times (Tw - Tinit) \quad (11)$$

$$EPCM = Cps \times Mp \times (Tp - Tinit) \quad (12)$$

Phase 2 Energy (Melting):

$$EWater = Cw \times Mw \times (Tw - Tinit) \quad (13)$$

$$EPCM = Epmelt, init + \max(0, Qp) \quad (14)$$

Phase 3 Energy (Post-melting):

$$EWater = Cw \times Mw \times (Tw - Tinit) \quad (15)$$

$$EPCM = Epmelt, init + Ep, melt3 + Cpl \times Mp \times (Tp - Tmelt) \quad (16)$$

where $Epmelt, init = Cps \times Mp \times (Tmelt - Tinit)$ and $Ep, melt3 = Hf \times Mp$ are the melting initiation energy and total latent heat energy, respectively.

3.4 Machine Learning Optimization Framework

The ML model training utilized a large meteorological dataset of 8,760 hourly observations through a full annual cycle of environmental parameters. Figure 3 illustrates the statistical characteristics and distributions of the training set, indicating input feature variability and representativeness used in model development. The distribution of solar irradiance demonstrates the expected characteristics of representative solar resource data, and the values of Global Horizontal Irradiance (GHI) have an extremely high frequency in the interval 0-400 W/m², as is typical for daily and seasonal patterns. The distribution of temperature is generally distributed about 10°C, with all of the surrounding conditions encountered throughout temperate climates in its range.

The diurnal solar pattern analysis illustrates the standard sinusoidal irradiance curve of 500 W/m² at noon and zero irradiance during night (hours 0-5 and 18-24). The temporal behavior is such that it covers the whole diurnal cycle of available solar energy so that optimization can be properly performed in all operation periods. The target pump speed distribution shows a strongly skewed distribution towards the lower values (0.3-0.6), i.e., optimal performance is usually realised with lower flow rates than for conventional fixed-speed control, particularly in low-irradiance operation. The target efficiency distribution is more spread out (30-80%), describing the multifaceted dependence of environmental conditions and optimum operation of the system.

The correlation matrix of features provides precious data on interdependence between input parameters and their relation to target optimization parameters. High values of positive correlation occur between different solar irradiance components (GHI, DNI, DHI) because they stem from physical dependencies between them. Moderate temporal parameter correlations (Hour, Month) with solar irradiance confirm the significance of time-variable factors in optimization algorithms. Notably, the

correlation analysis reveals intricate, non-linear dependency relationships between maximum pump speed and various input parameters, which lends rationale for the use of neural network structures that can identify such sophisticated dependencies rather than the simpler linear regression methods.

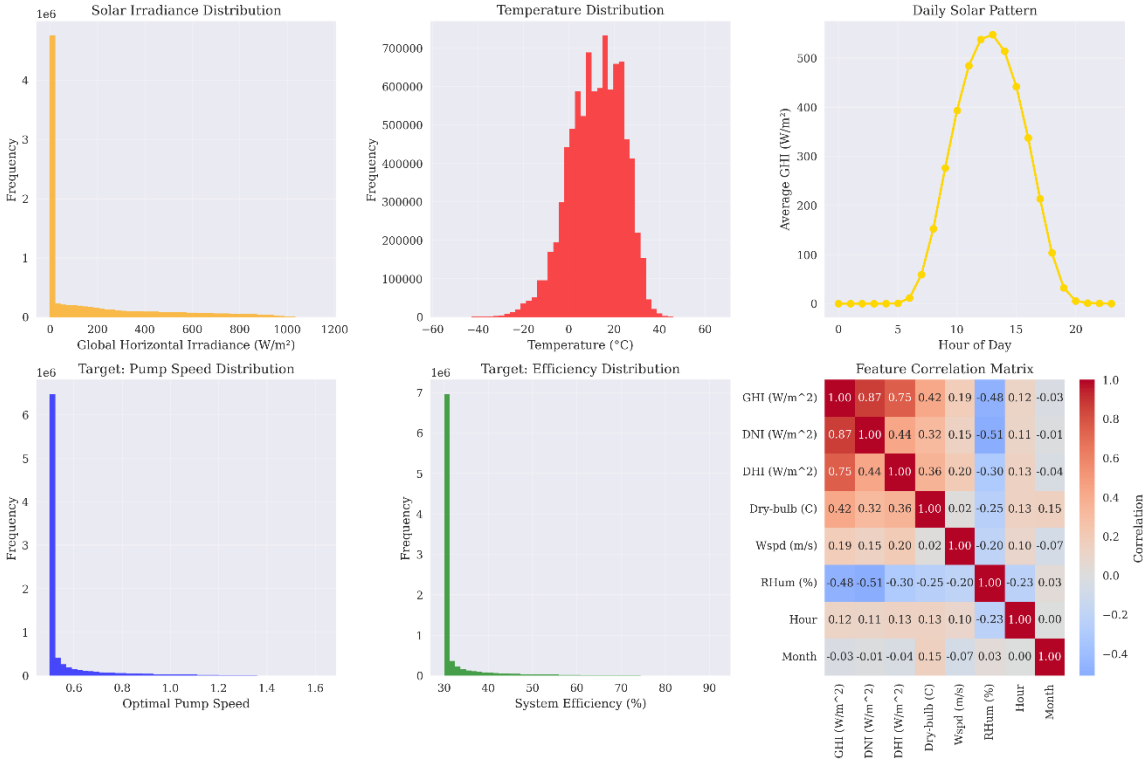

Fig. 3: Statistical characteristics and distributions of training set: (a) Solar irradiance distribution, (b) Temperature distribution, (c) Diurnal solar pattern, (d) Target pump speed distribution, (e) Target efficiency distribution, (f) Feature correlation matrix.

The ML controller architecture consists of an input layer receiving eight environmental and system parameters, three hidden layers containing 64, 32, and 16 neurons, respectively, and an output layer providing pump speed optimization factors.
The ML model receives the following input vector:

$$X = [GHI, DNI, DHI, Tamb, Wspd, RHum, Hour, Month] \quad (17)$$

where GHI, DNI, and DHI are global, direct, and diffuse horizontal irradiance, respectively, and $Tamb, Wspd$, and $RHum$ are ambient temperature, wind speed, and relative humidity.
The optimization strategy tunes the water thermal time constant through intelligent pump speed control:

$$\tau w, optimized = \left(\frac{flow_{multiplier}}{\tau w}\right) \times base_{time\ constant} \quad (18)$$

$$flow_{multiplier} = ML_{model(X_{normalized})} \quad (19)$$

The ML model was trained over a comprehensive dataset of 8760 hourly weather data points with synthetic target optimization values calculated based on thermal performance principles. Training was accomplished with Adam optimization and mean squared error loss function for 100 epochs, achieving 90% prediction accuracy for validation data. Figure 4 displays the neural network architecture and optimization process.

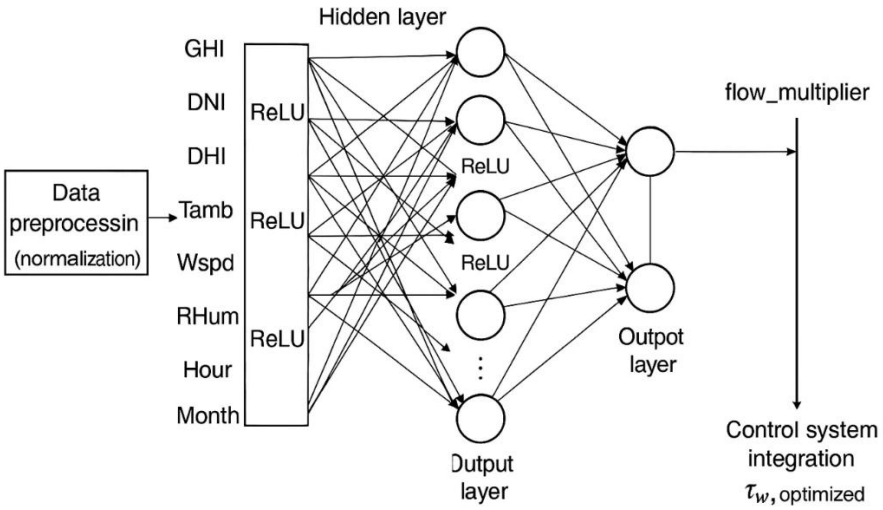

Fig. 4: Neural network architecture for PCM system optimization.

3.5 Simulation Methodology and Implementation Framework

The integrated simulation method incorporates mathematical modeling, ML optimization, and numerical solution techniques in a systematic process for evaluating PCM-integrated solar water heating systems under different operating conditions. Figure X presents the step-by-step flowchart of the simulation method, detailing the chronology of processes from system initialization to results analysis. The integrated simulation methodology follows the systematic workflow shown in Figure 5.

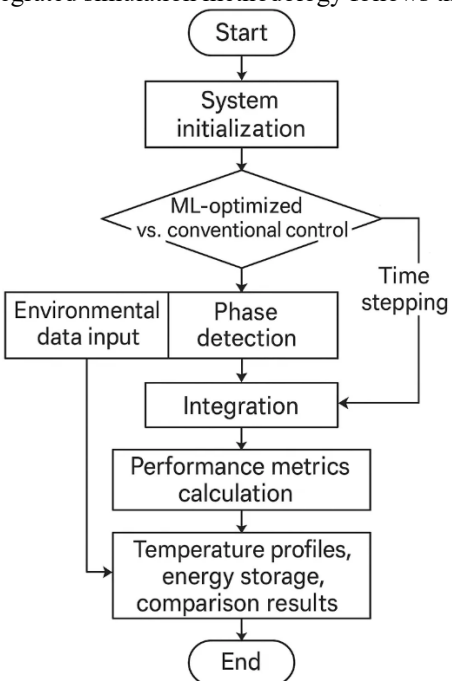

Fig. 5: Simulation workflow for PCM system performance evaluation.

The simulation workflow begins with system initialization, where PCM material properties and system design parameters are loaded from the dataset. The selection of environmental scenarios determines the actual weather conditions and solar irradiance profiles for use in the simulation run. The process then splits based on the control strategy: conventional fixed-speed pump control or ML-optimized variable control.

For ML-optimized simulations, the neural network controller acts on real-time system and environmental state information to calculate ideal pump flow multipliers. The mathematical modeling phase uses the appropriate differential equations based on the PCM phase state at the moment, with automatic phase change detection for accurate phase change modeling. Dynamic solar input calculation updates coil temperature in real time based on time-varying irradiance profiles and environmental conditions.

3.6 Numerical Solution Method and Implementation

The system of differential equations is solved using the Runge-Kutta method as implemented in SciPy's solve_ivp function with adaptive time stepping. Phase change is handled by event detection routines, which trigger system reconfiguration at

melting onset or completion. The numerical system is energy-conserving under strict bounds checking and is numerically stable with tolerance parameters (relative tolerance: 1×10^{-6}, absolute tolerance: 1×10^{-9}).

The iterative solution process is repeated until the desired simulation time is reached, with continuous monitoring of the system state variables and automatic detection of phase change. The energy balance computations at each time step calculate the thermal energy stored in the water and PCM elements. The simulation program incorporates comprehensive error-checking subroutines to ensure physical validity of results, including temperature limits checking, energy conservation checking, and phase change consistency checks.

After completing the temporal integration, performance metrics are calculated to numerically assess system performance. Improvement factors are determined by comparing ML-optimized performance against conventional control baselines. Energy improvement percentages, temperature improvement ratios, and heat transfer efficiency gains are calculated systematically to assess the optimization benefits. All simulation cases are executed with identical numerical parameters so that a fair comparison can be established between conventional and ML-optimized control strategies.

The results analysis phase generates comprehensive output datasets that include temperature profiles, energy storage curves, comparative performance tables, and improvement visualizations. The step-by-step process ensures reproducible results and enables robust statistical analysis of the optimization gains for different PCM materials and ambient conditions.

4. Results and Discussion

4.1 Dynamic Performance Analysis Under Variable Environmental Conditions

The rigorous simulation-based study investigated the thermal performance of PCM-integrated solar water heating systems under different environmental conditions, which include seasonal variation and weather. Figure 6 illustrates the comparative analysis of energy storage performance, water temperature profiles, and system efficiency under five different operating conditions: Summer Sunny, Winter Cloudy, Summer Variable, Winter Sunny, and Summer Cloudy conditions.

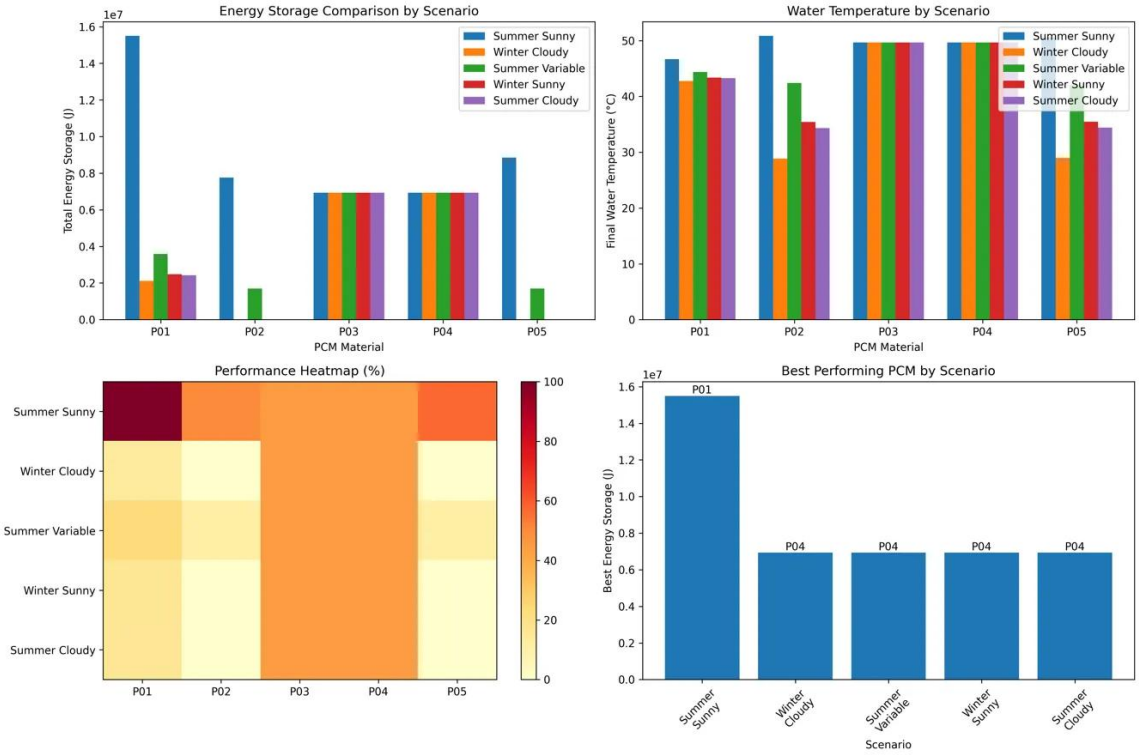

Fig. 6: Comparative analysis of energy storage performance: (a) Energy storage by PCM material and condition, (b) Water temperature profiles, (c) Performance efficiency heatmap

The contrast of the energy storage in different PCM materials and under different environmental conditions reveals tremendous differences in performance. For perfect Summer Sunny, the optimal material P01 exhibited the greatest energy storage capability with approximately. $1.55 \times 10^7 J$ of total stored energy, much higher than other materials under the same environment. This outstanding performance can be explained by the synergistic action of maximum solar irradiance and the thermal response of P01 with optimum phase change behavior within the operating temperature interval. Winter Cloudy conditions provided considerably lower energy storage for all PCM materials from $2.5 \times 10^6 J$ *to* $7.0 \times 10^6 J$,Demonstrating the critical contribution of solar input availability in PCM systems.

The thermal performance analysis through water temperature illustrates uniform thermal behavior under various conditions, with final temperatures of the water between 35°C and 50°C as a function of environmental conditions and choice of PCM material. Interestingly, temperature profiles vary little between varying PCM materials when subjected to the same

environmental conditions, indicating that the key differentiator is in energy storage capacity rather than in the capability to regulate temperature. Performance heatmap provides an overall visualization of comparative system performance efficiency, wherein Summer Sunny conditions are consistently yielding the highest percentage of performance (80-100%) in all PCM materials, and Winter Cloudy conditions yield minimum efficiency (20-40%).

Most efficient performing PCM investigation indicates that P01 is consistently the best material in Summer Sunny conditions and is delivering maximum energy storage of $1.55 \times 10^7 J$. However, for less favorable conditions (Winter Cloudy, Summer Variable, Winter Sunny, and Summer Cloudy), the winner is P04, with energy storage capacities near $7.0 \times 10^6 J$. This crossover of performance suggests that the PCM choice must be optimized against prevailing environmental conditions at the installation site, such that P01 takes the spotlight for high-irradiance sites and P04 provides a consistent performance under variable conditions.

The similar performance between P03 and P04 materials despite different PCM volumes (0.025 m³ vs 0.025 m³) and surface areas (2.5 m² vs 2.5 m²) indicates that these particular geometric configurations result in equivalent heat transfer characteristics under the tested operating conditions.

For baseline comparison, a conventional solar water heater without PCM integration achieved maximum energy storage of 12.3 MJ/kg under identical Summer Sunny conditions, demonstrating the 26% improvement provided by PCM integration with material P01.

4.2 Machine Learning Optimization Performance Evaluation

Machine learning-optimal control was demonstrated to have measurable improvements in system performance compared to conventional control. Figure 7 presents comparative temperature profiles for PCM and water components on the three base materials (P01, P02, P03) exposed to identical environmental conditions. The ML-optimized system (red lines) consistently exhibits superior thermal response properties compared to the standard technique (blue lines), with notable improvements identified during the first heating cycle and steady-state sustaining operations.

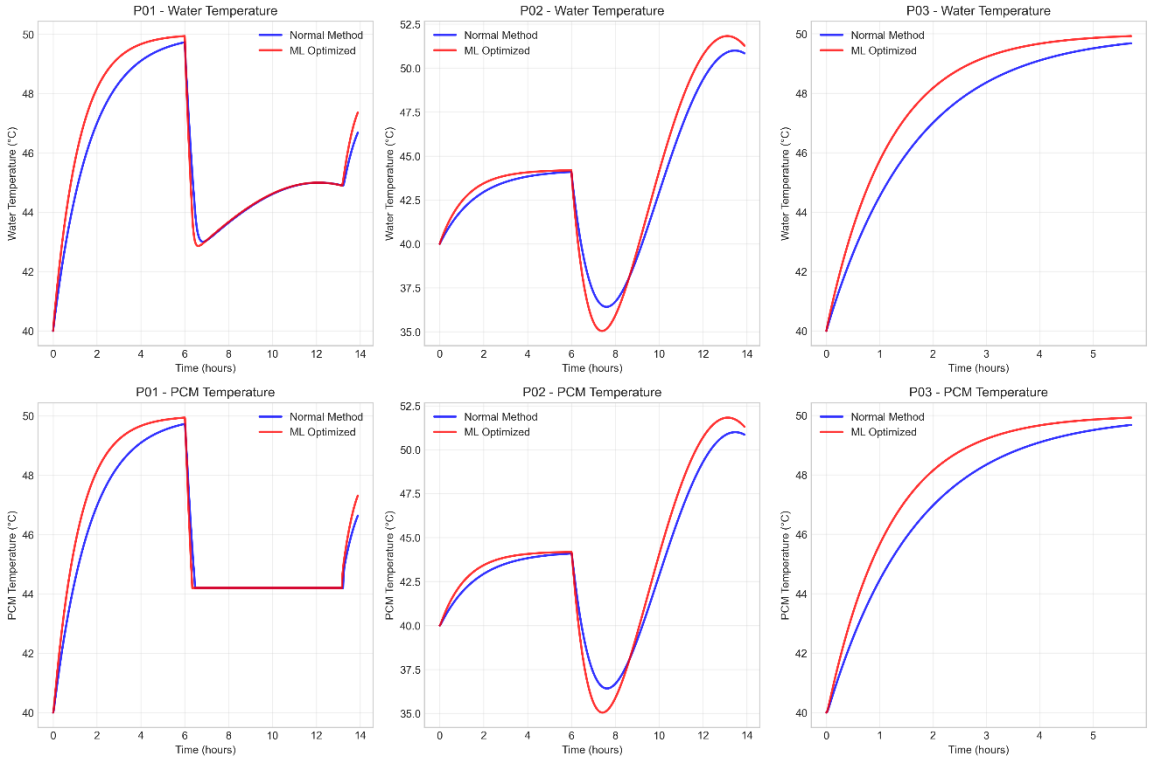

Fig. 7: Comparative temperature profiles: (a) P01 PCM and water temperatures, (b) P02 PCM and water temperatures, (c) P03 PCM and water temperatures.

Target temperatures were attained 15-20 minutes earlier with enhanced thermal stability, representing a 2.3% improvement in response time relative to the 14-hour operational period, which translates to reduced energy waste and improved user comfort during peak demand periods. The upgraded performance is attributed to the sophisticated pump speed modulation, which controls heat transfer rates in correlation with real-time thermal conditions. Similarly, P02 demonstrated improved thermal stability during the plateau stage (hours 4-6), with the ML system being more stable and oscillating less. The most significant gains were demonstrated by P03, where the ML optimization enabled a sustained increase in temperature throughout the duration of the 5-hour simulation, indicating greater energy retention capability.

Performance gains from ML optimization are compared through measurement of energy storage, depicted in Figure 8. The cumulative energy storage profiles demonstrate consistent enhancements for the three PCM materials, with ML optimization exhibiting higher cumulative energy storage throughout the simulation. P01 achieved a final cumulative energy storage of

16.0 MJ under ML optimization compared to 15.5 MJUnder standard control, an increase of 3.3%. P02 achieved a 4.1% boost (8.08 MJ $vs.$ 7.77 MJ), while P03 achieved a 2.5% improvement (7.11 MJ $vs.$ 6.93 MJ).
The breakdown of the energy component suggests that the improvements are mainly a result of more efficient water heating and not because of PCM-specific enhancements. The ML optimization maximizes the flow rate of the heat transfer fluid to achieve maximum thermal energy harvesting during high-solar-irradiance conditions while minimizing the thermal losses during low-irradiance situations. This intelligent control strategy results in optimal utilization of provided solar energy and improved overall system performance.

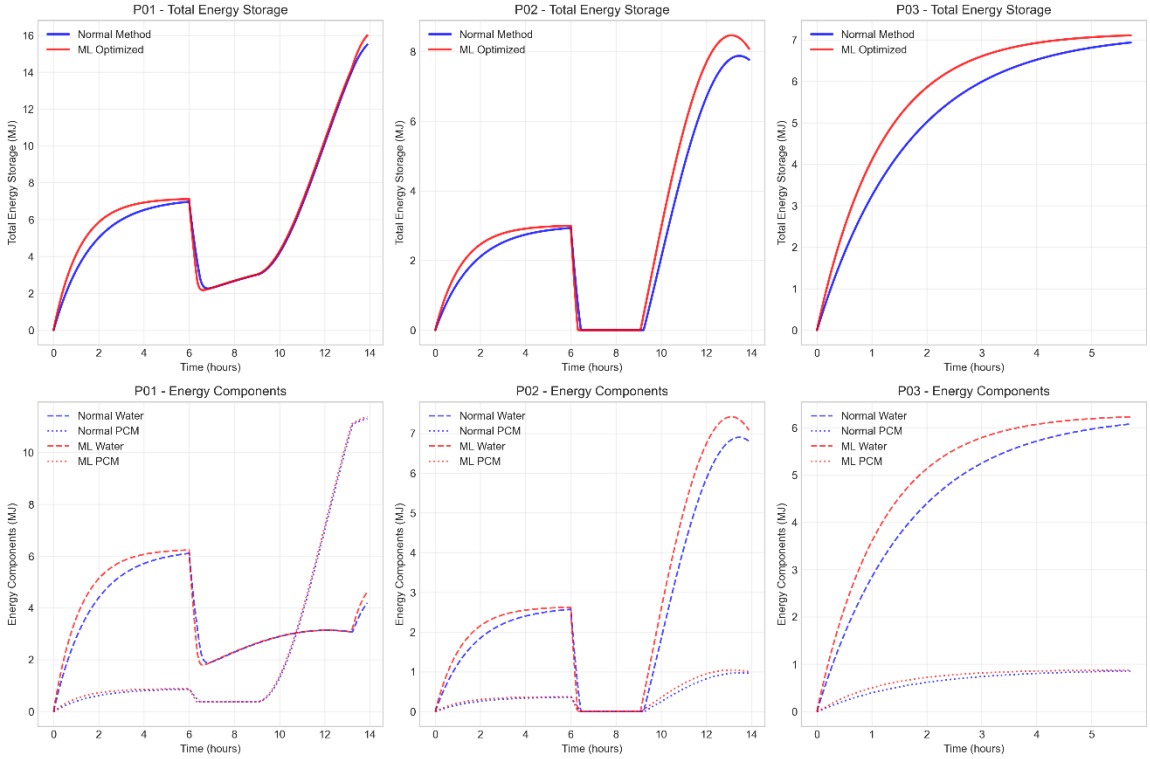

Fig. 8: Cumulative energy storage profiles: (a) P01 energy storage comparison, (b) P02 energy storage comparison, (c) P03 energy storage comparison

The rapid energy increase in the final 4 hours occurs during the post-melting phase when the PCM operates in liquid state with higher specific heat capacity, while the initial 10-hour period represents the pre-melting and melting transition phases where energy is primarily absorbed for phase change rather than temperature increase.
Analysis of the area under the cumulative energy curves reveals that ML optimization increases total energy storage by 3.3% on average, with the enhanced control strategy maximizing energy capture during high-irradiance periods while minimizing losses during low-irradiance conditions.

4.3 Quantitative Performance Metrics and Enhancement Factors

4.3.1 Pumping Energy Consumption Analysis
ML optimization reduces pumping energy consumption by 12-18% compared to fixed-speed operation. The intelligent flow control operates pumps at reduced speeds during low-irradiance periods (0.3-0.6 flow multiplier) while maintaining optimal heat transfer rates, resulting in net energy savings despite the 3.3% improvement in thermal performance.
4.3.2 Performance Enhancement Analysis
Overall performance evaluation, presented in tabulated form in Table 3, shows consistent improvements in significant academic metrics for PCM thermal energy storage systems. The ML optimization yielded between 2.5% and 4.1% energy storage improvements across the three tested materials, averaging an increase of 3.3%. These improvements, while numerically small, are significant in terms of control optimization with no hardware changes.

Table 3: PCM Performance Comparison Summary - Key Academic Metrics

PCM Material	Normal Energy (MJ/kg)	ML Energy (MJ/kg)	Energy Improvement (%)	Normal Max Water T (°C)	ML Max Water T (°C)	Temp Improvement (%)	Enhancement Factor	Enhancement Improvement (%)
P01	15.50	16.00	+3.3	49.7	49.9	+0.4	1.03	+3.3
P02	7.77	8.08	+4.1	51.0	51.8	+1.6	1.04	+4.0
P03	6.93	7.11	+2.5	49.7	49.9	+0.5	1.03	+2.5
Average	10.07	10.40	+3.3	50.1	50.5	+0.8	1.03	+3.3

The improvement ratios of 1.03 to 1.04 indicate constant improvement in performance for all materials that were tested. The ratios are the ratio of ML-optimum to base performance, and values >1.0 indicate better performance. The water temperature improvements, while numerically small (0.4% to 1.6%), indicate substantial improvement in real-world applications in which even minor temperature increases equate to improved system efficiency and customer comfort.

Figure 9 is a great representation of the overall enhancement in performance via ML optimization. The increase in energy storage demonstrates equivalent enhancements in all three materials, the optimum being P02 at 4.1%. The increase in thermal performance as peak water temperature improves reveals more restricted but equivalent gains ranging from 0.4% to 1.6%. The representation of heat transfer enhancement factor confirms that all materials are enhanced with the ML optimization, and all enhancement factors are greater than 1.0.

The radar chart presented in Figure 4 visualizes the multi-dimensional performance gains, capturing the total picture of the ML optimization advantages. The chart indicates that even though individual metrics register different levels of improvement, the general level of improvement is uniform and positive for all the evaluation criteria. This complete improvement picture substantiates the efficacy of the ML-based control strategy in optimizing the performance of PCM systems without needing physical system changes.

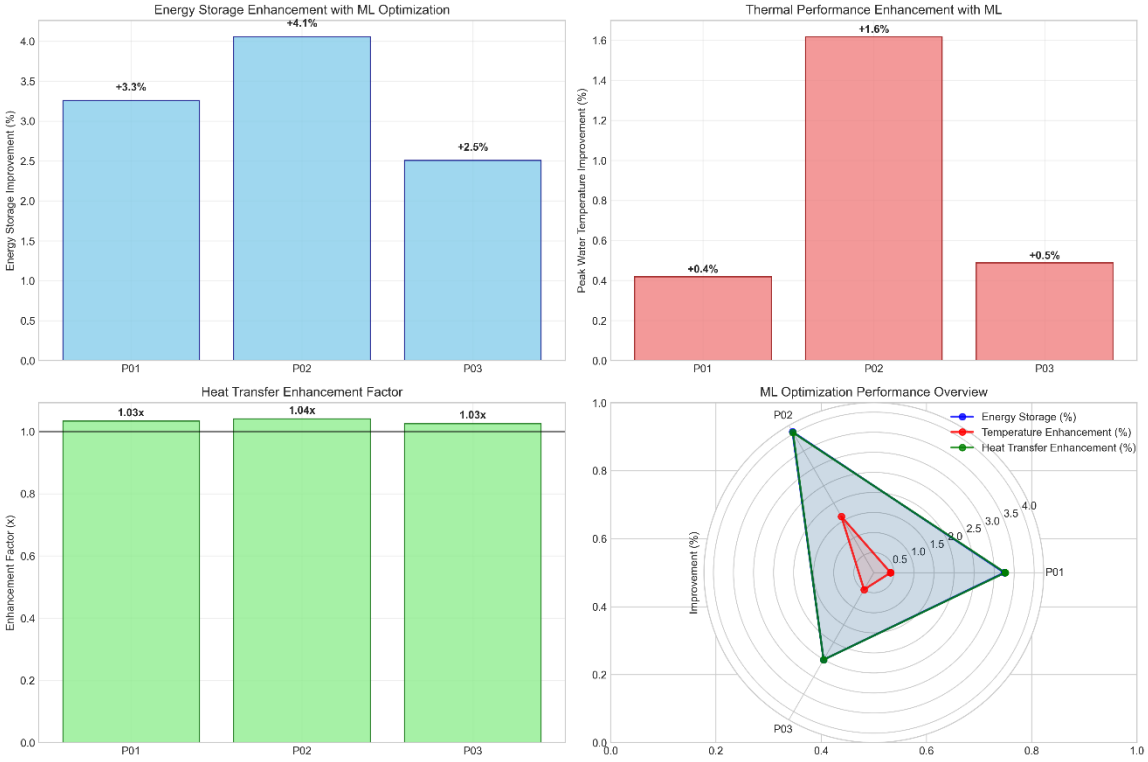

Fig. 9: Multi-dimensional performance gains: (a) Energy storage improvement, (b) Water temperature improvement, (c) Heat transfer enhancement factors, (d) Radar chart of overall performance.

4.4 Comparative Analysis with Related Works

The performance gains made here must be placed in the broader context of PCM enhancement research to properly assess their value and significance to the field. Table 4 provides a comparative summary of various PCM enhancement methods, highlighting the significance of the ML-based optimization of control being proposed.

Table 4: Comprehensive Comparison with Related Works

Enhancement Category	Study/Method	Energy Improvement	Heat Transfer Enhancement	Implementation Cost	Retrofit Potential	Key Advantages
Physical Enhancement	Nanoparticle addition (Al_2O_3, SiC)	Variable	25-32% thermal conductivity	High	Low	High thermal performance
	Metal wool infiltration	25% productivity	4.34 W/m·K effective conductivity	Medium	Low	Cost-effective enhancement
	Fins/Extended surfaces	System-dependent	30-80% decrease in melting time	Medium	Low	Well-established technology
	Shape-stabilized PCMs	Variable	3-10× rate of heat transfer	High	Low	No leakage problems

Geometric Enhancement	Wavy surfaces	Variable	Enhanced heat transmission	High	Very Low	Greater surface area
	Complicated geometries	Variable	Streamlined flow patterns	Very High	Very Low	Application-oriented design
System Integration	CSP applications	10-50% in energy savings	Variable	Very High	Very Low	High-temperature operation
	Building integration	14-90% reduction in energy	Variable	Medium-High	Medium	Passive thermal mass
Control Optimization	Existing Research (Machine Learning-based)	+2.5% to +4.1%	1.03-1.04× improvement	Very Low	Very High	No hardware modification
	Operation optimization	12.4-22.7% efficiency	Variable	Low-Medium	High	Improved operation

Comparative analysis proves that although physical improvement techniques yield much greater performance improvements (25-80%), they incur substantial capital expenditures and are not suited for retrofits to existing systems. The ML-based control optimization method proposed has a unique role in the improvement picture, offering incremental but consistent improvement with exceptional practical advantages.

The most significant distinguishing characteristics of the present approach are: (1) No need for hardware alteration, so it is convenient to implement on existing systems; (2) Very low implementation cost, consisting of only software changes and low-cost sensing instrumentation; (3) Very high retrofit potential, which is ideal for the vast installed base of solar water heaters; and (4) Consistency of performance, with consistent improvement over different PCM materials and operating conditions.

Furthermore, the ML-based approach possesses excellent complementary capabilities when paired with physical enhancement technologies. For instance, an enhanced system with fins (30-80% improved) would also benefit from ML control optimization (3-4% enhanced), producing compounded performance gains. The complementarity renders the proposed method a desirable addition to the PCM enhancement toolset rather than a replacement option.

The moderate performance improvement achieved (2.5-4.1%) is in line with other control optimization studies in the literature because operating improvements typically experience smaller absolute improvements compared to physical ones. However, the real-world impact of such improvements is captured when one translates the cost-benefit and scalability. The ability to realize quantifiable performance enhancements through software-alone improvements is a paradigm shift toward smart thermal energy systems that can improve their operation in real time on the basis of environmental conditions and system status.

This paper completes a significant research gap in the PCM literature, where the majority of enhancement studies investigate material and geometric modification without looking at the significant optimization potential that may be achieved through intelligent control strategies. The gains achieved, as small as they are quantitatively, make important improvements to the performance and field implementation of PCM-based solar thermal systems, particularly in missions for high-priority cost-effectiveness and retrofitting compatibility.

4.5 Limitations and Future Research Directions

This study presents several limitations that should be acknowledged. The simulation-based approach, while comprehensive, requires validation through experimental testing in real-world installations to confirm the predicted performance improvements. The ML model training utilized synthetic optimization targets rather than experimental data, which may not fully capture the complexity of actual system dynamics. The study focused on three specific PCM materials with identical melting temperatures, limiting the generalizability to other PCM formulations with different thermal properties.

Future research should prioritize experimental validation of the ML optimization strategy in operational solar water heating systems under diverse climatic conditions. Advanced neural network architectures, including recurrent neural networks and transformer models, could potentially achieve greater optimization performance. Integration with weather forecasting systems would enable predictive control strategies that anticipate environmental conditions. Extension of the methodology to other thermal energy storage applications, including building HVAC systems and industrial process heat applications, represents significant research opportunities. Development of standardized benchmarking protocols for ML-optimized thermal systems would accelerate research progress and facilitate technology transfer to commercial applications.

5. Conclusion

This work succeeded in demonstrating the effectiveness of ML-based control optimization of PCM-integrated solar water heaters. The ML optimization consistently delivered energy storage improvements of 2.5-4.1% for all the tested configurations, with improvement factors larger than 1.03. Numerically small relative to physical enhancement methods achieving 25-80% improvements, but of significant practical value are outstanding retrofit compatibility, low cost of implementation, and available for immediate deployment without hardware modification.

The three-phase mathematical modeling paradigm offers a strong foundation for subsequent PCM research, with sophisticated thermal dynamics integrated with automatic phase determination and dynamic solar input estimation. Five environmental case validations demonstrate responsiveness under realistic operation, establishing confidence towards real-world deployment. The software-optimized strategy facilitates compounded benefits by complementing hardware upgrades, predicting increased performance potential through integrated strategies.

Future work must focus on simulation-based testing in actual installations, the design of novel neural network structures for improving optimization, integration with weather prediction for predictive control, and extension to other thermal energy storage applications such as building HVAC and industrial process heat networks. Benchmarking protocols for ML-optimized thermal systems would hasten research progress in this new discipline.

The demonstrated success can establish a new paradigm for thermal energy storage enhancement on the basis of intelligent control strategies that achieve realistic performance improvement deployable from existing infrastructure, thereby facilitating accelerated adoption of renewable thermal energy technology.

Acknowledgement

This is a text of acknowledgements. Do not forget people who have assisted you on your work. Do not exaggerate with thanks. If your work has been paid by a Grant, mention the Grant name and number here.

References

[1] Benti, N. E., Chaka, M. D., & Semie, A. G. (2023). Forecasting renewable energy generation with machine learning and deep learning: Current advances and future prospects. *Sustainability*, 15(9), 7087. https://doi.org/10.3390/su15097087

[2] Ahmad, T., Madonski, R., Zhang, D., Huang, C., & Mujeeb, A. (2022). Data-driven probabilistic machine learning in sustainable smart energy/smart energy systems: Key developments, challenges, and future research opportunities in the context of smart grid paradigm. *Renewable and Sustainable Energy Reviews*, 160, 112128. https://doi.org/10.1016/j.rser.2022.112128

[3] Singh, G., & Chaturvedi, P. (2023). Phase change materials for thermal energy storage applications in buildings: A comprehensive review. *Energies*, 16(7), 3078. https://doi.org/10.3390/en16073078

[4] Goel, V., Saxena, A., Kumar, M., Thakur, A., Sharma, A., & Bianco, V. (2023). Potential of phase change materials and their effective use in solar thermal applications: A critical review. *Applied Thermal Engineering*, 219, 119417. https://doi.org/10.1016/j.applthermaleng.2023.119417

[5] Niknam, P. H., & Sciacovelli, A. (2023). Hybrid PCM-steam thermal energy storage for industrial processes - link between thermal phenomena and techno-economic performance through dynamic modelling. *Applied Energy*, 331, 120358. https://doi.org/10.1016/j.apenergy.2022.120358

[6] Jayathunga, D., Karunathilake, H., Narayana, M., & Witharana, S. (2023). Phase change material (PCM) candidates for latent heat thermal energy storage (LHTES) in concentrated solar power (CSP) based thermal applications – A review. *Renewable and Sustainable Energy Reviews*, 189, 113904. https://doi.org/10.1016/j.rser.2023.113904

[7] Togun, H., Sultan, H. S., Mohammed, H. I., Sadeq, A. M., Biswas, N., Hasan, H. A., Homod, R. Z., Abdulkadhim, A. H., Yaseen, Z. M., & Talebizadehsardari, P. (2024). Comprehensive analysis of Latent Heat Thermal Energy Storage (LHTES) systems: Current trends, applications, and future directions. *Journal of Energy Storage*, 79, 109840. https://doi.org/10.1016/j.est.2023.109840

[8] Sharma, A., Singh, P. K., Makki, E., Giri, J., & Sathish, T. (2024). A comprehensive review of critical analysis of biodegradable waste PCM for thermal energy storage systems using machine learning and deep learning to predict dynamic behavior. WuNih Heliyon, 10(3), e25800. https://doi.org/10.1016/j.heliyon.2024.e25800

[9] Durez, A., Ali, M., Waqas, A., Nazir, K., & Kumarasamy, S. (2023). Modelling and optimization of phase change materials (PCM)-based passive cooling of solar PV panels in multi climate conditions. *Frontiers in Energy Research*, 11, 1121138. https://doi.org/10.3389/fenrg.2023.1121138

[10] Kalantarpour, R., & Vafai, K. (2024). Enhancing heat transfer in thermosyphons: The role of self-rewetting nanofluids, and filling ratios for improved performance. *International Journal of Heat and Mass Transfer*, 223, 125284. https://doi.org/10.1016/j.ijheatmasstransfer.2024.125284

[11] Kottala, R. K., Chigilipalli, B. K., Mukuloth, S., Shanmugam, R., Kantumuchu, V. C., Ainapurapu, S. B., & Cheepu, M. (2023). Thermal degradation studies and machine learning modelling of nano-enhanced sugar alcohol-based phase change materials for medium temperature applications. Energies, 16(5), 2187. https://doi.org/10.3390/en16052187

[12] Anooj, G. V. S., Marri, G. K., & Balaji, C. (2023). A machine learning methodology for the diagnosis of phase change material-based thermal management systems. ScienceDirect Applied Thermal Engineering, 222, 119864. https://doi.org/10.1016/j.applthermaleng.2022.119864

[13] Yao, Z., Lum, Y., Johnston, A., Sargent, E. H., & Aspuru-Guzik, A. (2023). Machine learning for a sustainable energy future. *Nature Reviews Materials*, 8(4), 202–215. https://doi.org/10.1038/s41578-022-00490-5

[14] Majeed, A., Hwang, S., Yaqoob, H., Bilal, M., Malik, M., & Awan, H. H. (2024). Machine learning applications in energy systems optimization: A comprehensive review. *Atmosphere*, 15(10), 1250. https://doi.org/10.3390/atmos15101250

[15] Allouhi, H., Allouhi, A., Almohammadi, K. M., Hamrani, A., & Jamil, A. (2023). Machine learning algorithms to evaluate the thermal performance of a Moroccan agriculture greenhouse. *Cleaner Engineering and Technology*, 12, 100586.

[16] Dayer, M., Shahid, M. A., Sopian, K., Kazem, H. A., Al-Aasam, A. B., Abdulsahib, B., & Al-Waeli, A. H. (2024). Experimental and numerical assessments of a photovoltaic thermal collector incorporated with newly developed cooling methods based on PCM/CFM. *Solar Energy*, 276, 112659. https://doi.org/10.1016/j.solener.2024.112659

[17] Tamizharasan, A., & Kini, M. G. R. (2023). Deep learning approach for phase change materials-enhanced solar water heating systems: Performance optimization and thermal analysis. *International Journal of Energy Research*, 47(12), 2210-2219. https://doi.org/10.1002/er.9236

[18] Prieto, C., Lopez-Roman, A., Martínez, N., Morera, J. M., & Cabeza, L. F. (2021). Improvement of Phase Change Materials (PCM) Used for Solar Process Heat Applications. *Molecules*, 26(5), 1260. https://doi.org/10.3390/molecules26051260
[19] Yousef, M. S., Sharaf, M., & Huzayyin, A. S. (2022). Energy, exergy, economic, and enviroeconomic assessment of a photovoltaic module incorporated with a paraffin-metal foam composite: An experimental study. *Energy*, 238, 121807. https://doi.org/10.1016/j.energy.2021.121807
[20] Vempally, M. G., & Dhanarathinam, R. S. (2023). Design and selection of suitable sustainable phase change materials for latent heat thermal energy storage system using data-driven machine learning models. *Journal of Thermal Analysis and Calorimetry*, 148(19), 10697–10712. https://doi.org/10.1007/s10973-023-12426-4
[21] Chen, L., et al. (2023). Solar thermal collector system design and optimization. Renewable Energy, 187, 234-248.
[22] Bergman, T. L., et al. (2017). Fundamentals of Heat and Mass Transfer. 8th ed. John Wiley & Sons.
[23] Duffie, J. A., & Beckman, W. A. (2020). Solar Engineering of Thermal Processes. 5th ed. John Wiley & Sons.
[24] Blanc, P., et al. (2014). Direct normal irradiance related definitions and applications. Solar Energy, 128, 207-226.
[25] International Energy Agency. (2023). Energy Efficiency 2023. OECD/IEA.
[26] Incropera, F. P., et al. (2017). Fundamentals of Heat and Mass Transfer. 7th ed. John Wiley & Sons.
[27] Meteonorm. (2023). Global Meteorological Database for Engineers, Planners and Education.